Biochemistry
Cite This: Biochemistry 2018, 57, 4741−4746
From the Bench
pubs.acs.org/biochemistry

# Dynamic Nuclear Polarization Nuclear Magnetic Resonance in Human Cells Using Fluorescent Polarizing Agents

Brice J. Albert,[†] Chukun Gao,[†] Erika L. Sesti,[†] Edward P. Saliba,[†] Nicholas Alaniva,[†] Faith J. Scott,[†] Snorri Th. Sigurdsson,[‡] and Alexander B. Barnes*[,†]

[†]Department of Chemistry, Washington University in St. Louis, One Brookings Drive, St. Louis, Missouri 63130, United States
[‡]University of Iceland, Department of Chemistry, Science Institute, Dunhaga 3, 107 Reykjavik, Iceland

Supporting Information

**ABSTRACT:** Solid state nuclear magnetic resonance (NMR) enables atomic-resolution characterization of the molecular structure and dynamics within complex heterogeneous samples, but it is typically insensitive. Dynamic nuclear polarization (DNP) increases the NMR signal intensity by orders of magnitude and can be performed in combination with magic angle spinning (MAS) for sensitive, high-resolution spectroscopy. Here we report MAS DNP experiments, for the first time, within intact human cells with >40-fold DNP enhancement and a sample temperature of <6 K. In addition to cryogenic MAS results at <6 K, we also show in-cell DNP enhancements of 57-fold at 90 K. In-cell DNP is demonstrated using biradicals and sterically shielded monoradicals as polarizing agents. A novel trimodal polarizing agent is introduced for DNP, which contains a nitroxide biradical, a targeting peptide for cell penetration, and a fluorophore for subcellular localization with confocal microscopy. The fluorescent polarizing agent provides in-cell DNP enhancements of 63-fold at a concentration of 2.7 mM. These experiments pave the way for structural characterization of biomolecules in an endogenous cellular context.

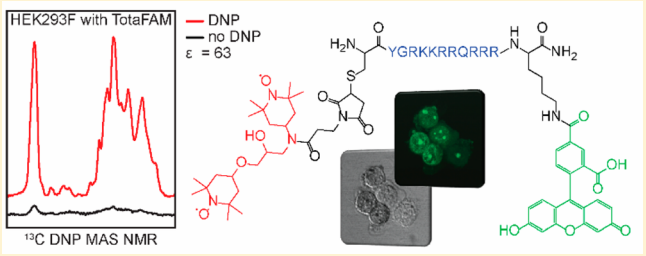




Solid state nuclear magnetic resonance (NMR) is exquisitely suited to characterization of molecular structure within endogenous environments, including in cells.[1−5] However, the concentration of target biomolecules in these complex preparations is much lower than that in highly purified samples, challenging the sensitivity limit of NMR spectroscopy. Strategies for increasing NMR sensitivity are, therefore, an important aspect of improving solid state NMR and in-cell NMR spectroscopy. In-cell NMR experiments typically involve exogenous protein expression in cells or otherwise increasing target protein concentrations beyond endogenous levels and can result in sufficient NMR sensitivity.[6−9] However, such perturbations alter endogenous biomolecular interactions and their associated pathways. Alternatively, increasing NMR sensitivity by multiple orders of magnitude will permit in-cell structural characterization of biomolecules at endogenous concentrations.

Strategies for increasing NMR sensitivity include access to high static magnetic fields,[10,11] cryogenic sample temperatures,[12] more sensitive detection schemes,[13] and spin polarization transfers.[14] Such polarization transfer mechanisms most effectively increase NMR sensitivity when the transferring spin has the highest spin polarization. Dynamic nuclear polarization (DNP) utilizes electron spins as the originating polarization source.[15,16] Cryogenic operation (<6 K), high static magnetic fields (>7 T), and efficient DNP transfers can result in high NMR polarization and >10000-fold increases in the intensities of NMR signals.[17] DNP has been successful at polarizing the outer membrane and cell wall of bacteria[18−20] but has not been demonstrated within bacteria, most likely because of the poor bacterium−cell permeability of DNP polarizing agents. Furthermore, magic angle spinning (MAS) DNP has yet to be extended to studies of human cells. Performing DNP *in situ* within intact cells has many advantages, including repeating experiments quickly for NMR signal averaging and determining the subcellular localization of NMR signals. Here we demonstrate in-cell DNP NMR in intact human cells and characterize the signal enhancements obtained using biradicals, sterically shielded monoradicals, and a novel trimodal fluorescent polarizing agent. The fluorescent DNP polarizing agent is comprised of a nitroxide biradical, a targeting peptide for cell penetration, and a fluorophore for subcellular localization with confocal microscopy.

## MATERIALS AND METHODS

Forty million intact human embryonic kidney cells (HEK293F), grown in Dulbecco's modified Eagle's medium (DMEM) supplemented with [U-$^{13}$C]glucose, were collected from a cell culture and spun down at 300*g* for 2 min. Cells were washed with 4 mL of natural abundance minimal essential medium (MEM) and spun down at 800*g* for 1 min. The resulting cell pellet was suspended with 100 $\mu$L of natural abundance MEM

Special Issue: Discovering New Tools
Received: March 1, 2018
Revised: June 15, 2018
Published: June 20, 2018




DOI: 10.1021/acs.biochem.8b00257
Biochemistry 2018, 57, 4741−4746

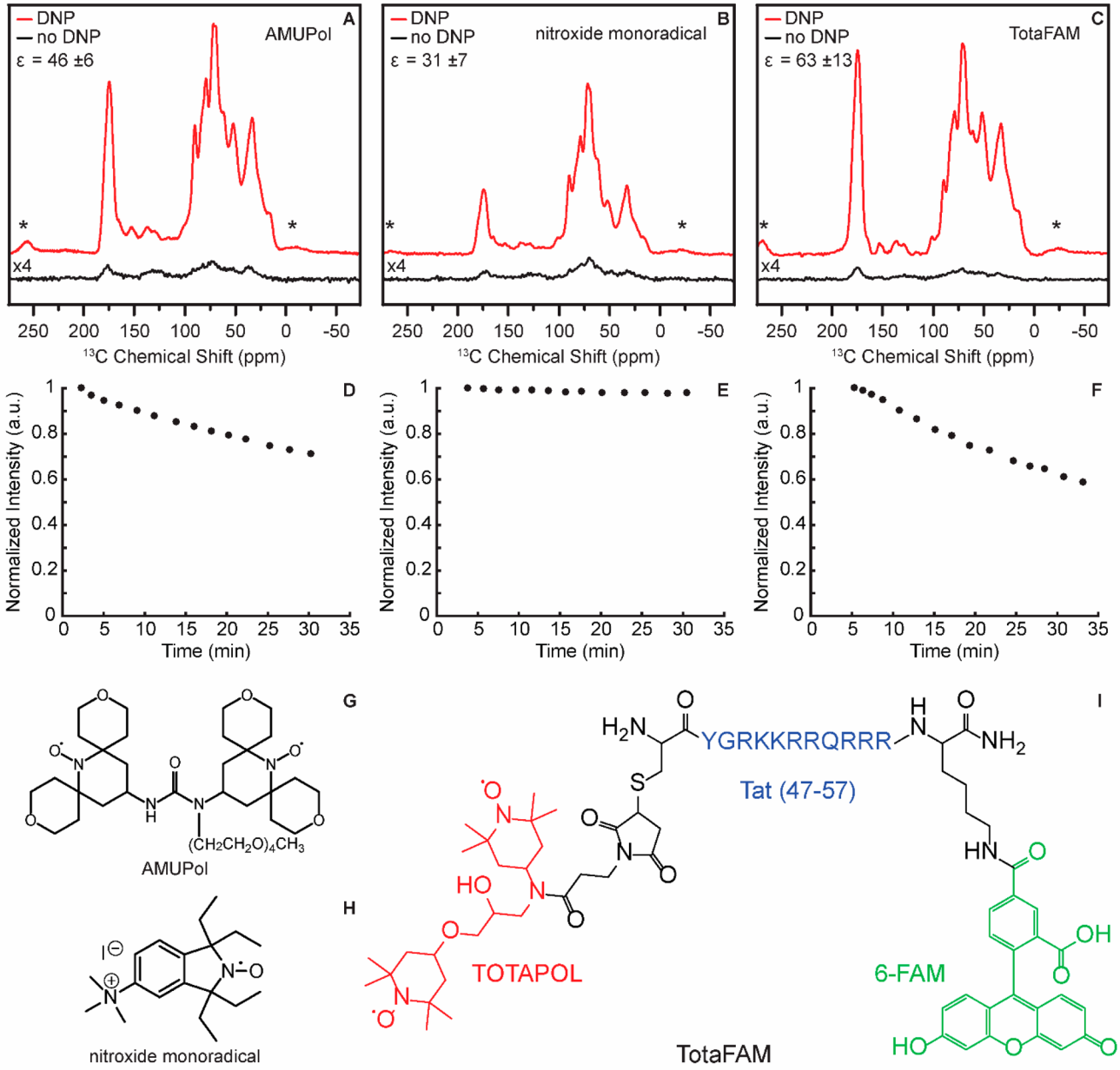


**Figure 1.** Characterization of nitroxide radicals in HEK293F cells. DNP CPMAS NMR spectra at <6 K using (A) 20 mM AMUPol, (B) 40 mM sterically shielded nitroxide monoradical, and (C) 2.7 mM TotaFAM. Black spectra were recorded without microwave irradiation, while red spectra were recorded with microwave irradiation. Asterisks denote spinning side bands. The $^{13}C$ resonances in the 50−100 ppm chemical shift range are attributed to sugars (Figure S9). Intensity of integrated EPR spectra vs time of cellular samples prepared with (D) AMUPol, (E) sterically shielded nitroxide monoradical, and (F) TotaFAM. Polarizing agents (G) AMUPol, (H) sterically shielded nitroxide monoradical, and (I) trimodal polarizing agent, TotaFAM. The three moieties of TotaFAM include a TOTAPOL nitroxide radical (red), 11 residues of the HIV-1 Tat protein (blue), and a 6-FAM fluorophore (green).

(containing 10% dimethyl sulfoxide) with DNP radical (20 mM, 2.7 mM AMUPol, 2.7 mM TotaFAM, and 40 mM nitroxide monoradicals[21]). Of the suspended cell volume, 80 $\mu$L was aliquoted for DNP NMR, 40 $\mu$L for electron paramagnetic resonance (EPR) characterization, and 2 $\mu$L for microscopy. Finally, samples were spun, at 800*g* for 30 s, directly into NMR rotors or EPR tubes. The supernatant from samples was removed, and the samples were frozen immediately in a liquid nitrogen bath. The total time taken for sample packing, defined as the time from when radicals were added to the cell suspension to when samples were frozen, ranged from 1 to 2 min. Sample masses packed into NMR rotors fell in a range of 32−35 mg, containing 15−20 million cells. Samples were stored at −80 °C (see further experimental details in Supplementary Section 4).

DNP experiments at $B_0$ = 7.05 T (300.184 MHz $^1H$) were performed with a custom-built MAS NMR probe housing 3.2 mm outside diameter rotors[22] and a frequency-agile gyrotron.[23] Spectra were recorded with a rotor-synchronized, echo-detected cross-polarization (CP) MAS pulse sequence (Figure S1). To destroy residual polarization, saturation trains (SAT) were implemented before a DNP polarization time ($\tau_{pol}$) and the CPMAS sequence, resulting in a SAT−$\tau_{pol}$−CPMAS overall sequence. A microwave irradiation frequency of 197.674 GHz was used for cross-effect polarization transfer from nitroxide



DOI: 10.1021/acs.biochem.8b00257
*Biochemistry* 2018, 57, 4741−4746

radicals. See the Supporting Information for more experimental details.

## RESULTS AND DISCUSSION

**In-Cell NMR with Biradicals and Monoradicals.** Magic angle spinning (MAS) NMR spectra of intact human embryonic kidney cells (HEK293F) were enhanced through DNP using both biradicals and monoradicals at sample temperatures of <6 K and also at 90 K. We found that nitroxide biradicals and monoradicals effectively enhanced HEK293F carbon signals through DNP and cross-polarization. The nitroxide biradical, AMUPol (Figure 1G),[24] yielded an enhancement of 46 within intact human cells (Figure 1A). Note that preliminary experiments that included a washing step after incubation of the polarizing agent did not show significant DNP enhancements.

Sterically shielded nitroxide monoradicals (Figure 1H), which are less prone to radical reduction in cellular environments,[21] also provided a significant DNP enhancement of 31 (Figure 1B). To compare enhancements from nitroxides, concentrations were kept constant at 20 mM for biradicals and 40 mM for monoradicals. We note that the proton longitudinal relaxation time under microwave irradiation ($T_{1\_DNP}$) was <3 s for HEK293F samples prepared with nitroxide radicals (Figure S11). This permitted fast repetition of scans and reduced the time needed for signal averaging. DNP enhancements of 57 from intact human cells were also observed at 90 K (see Figure 2).

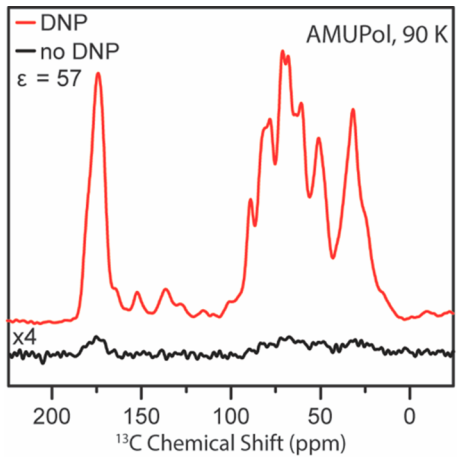


**Figure 2.** DNP CPMAS NMR of HEK293F cells at 90 K. $^{13}C$ DNP spectra recorded at 90 K of cells washed with phosphate-buffered saline (PBS) and suspended in PBS with 20 mM AMUPol. Black spectra were recorded without microwave irradiation, while red spectra were recorded with microwave irradiation.

EPR spectroscopy of nitroxide biradicals at room temperature, after incubation with HEK293F cells, was performed to monitor radical reduction in the cellular environment (Figure 1D–F). After 30 min, a 30% loss of signal intensity was observed for the AMUPol nitroxide biradical (Figure 1D), while the sterically shielded monoradical signal loss was only 2.1% (Figure 1E). Combined with the successful DNP enhancements of >30, these results indicate radical reduction does not prevent in-cell applications of DNP. Nonetheless, our sample preparation protocol minimizes the exposure of radicals to the reducing environment of cells by quickly (<3 min) freeze-quenching the cellular preparations after addition of radicals. EPR measurements showed a <2% loss of the biradicals before the samples were frozen.

Nitroxide radicals showed mostly uniform enhancement over all resonances. However, $^{13}C$ resonances between 100 and 150 ppm exhibited particularly attenuated DNP enhancement (Figure S7). Additionally, differences in the signal intensities between the spectra shown in panels A and B of Figure 1 using different radicals suggest a heterogeneous cellular distribution of polarizing agents. To determine the distribution of the radicals, we synthesized a novel polarizing agent that includes a fluorophore to enable optical localization.

**In-Cell NMR with Trimodal DNP Polarizing Agents.** We designed a trimodal fluorescent DNP polarizing agent, coined TotaFAM, containing a binitroxide radical for cross-effect DNP, a Tat peptide for intracellular targeting, and a fluorophore for optical localization (Figure 1I). A maleimide-derived TOTAPOL[25] was conjugated to an N-terminal cysteine residue of the targeting cell-penetrating peptide, residues 47–57 of the HIV-1 Tat protein.[26,27] The lysine side chain on the C-terminus of the Tat peptide was covalently linked to fluorescein. In addition to cell penetration, the Tat peptide linker limits the proximity of the fluorophore to radicals to mitigate fluorescence quenching, while retaining molecular connectivity to enable optical localization of DNP polarizing agents. The TOTAPOL biradical moiety[28] on TotaFAM provided DNP enhancements of 63 within HEK293F cells (Figure 1C). As seen for the AMUPol degradation rate, EPR spectroscopy of the biradicals on TotaFAM indicates a 43% loss after 30 min within cells and a <3% loss during the sample preparation time of <3 min (Figure 1F).

The stability of the chemical linkages employed in TotaFAM within cellular environments,[29,30] in addition to the short time TotaFAM was exposed to degradation before freeze-quenching (<3 min), suggests that the biradical moiety remains covalently linked to the fluorophore. This new class of fluorescent DNP polarizing agents enables the correlation of subcellular localization determined via optical microscopy with chemical and structural information determined with DNP-enhanced in-cell NMR.

Confocal microscopy was used to confirm cellular uptake through fluorescence detection. Comparison of the differential interference contrast (DIC) image (Figure 3A) with the

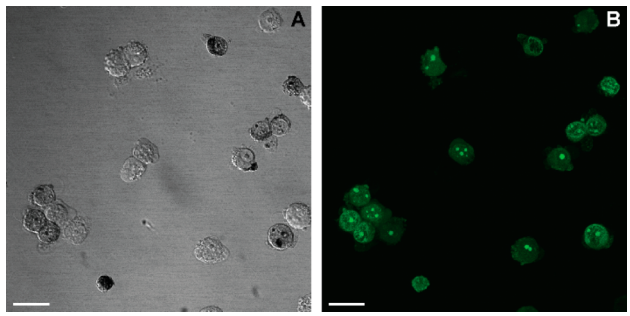


**Figure 3.** Confocal microscopy of a subset of a cellular culture that was used for DNP NMR experiments. Images confirm the cellular uptake of TotaFAM through comparison of (A) a DIC image and (B) a fluorescent image. The scale bar is 25 $\mu$m.

fluorescent image (Figure 3B) demonstrates cellular uptake of TotaFAM. Additionally, the fluorescent image shows that TotaFAM was not observed between cells.

To confirm the intracellular structures in which the TotaFAM accumulates, we performed additional microscopy using a nuclear



DOI: 10.1021/acs.biochem.8b00257
Biochemistry 2018, 57, 4741–4746

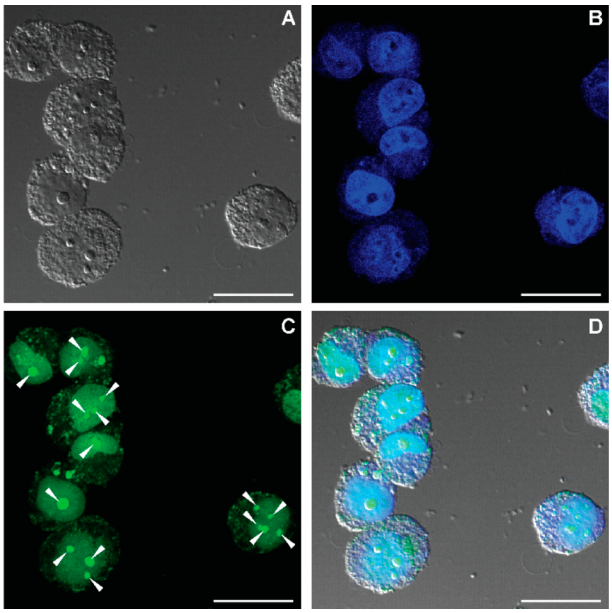


**Figure 4.** TotaFAM localizes to nucleoli of HEK293F cells. Confocal microscopy provided (A) a DIC image, (B) staining of nuclei with DAPI, (C) uptake of the trimodal polarizing agent, TotaFAM, and (D) an overlay of panels A–C. White arrows indicate nucleoli. The scale bar is 25 $\mu$m.

stain, DAPI. Figure 4 shows DIC and fluorescent micrographs of HEK293F cells post-incubation with TotaFAM, fixed with formaldehyde and subsequently stained with DAPI. Nucleoli have a low concentration of DNA and therefore bind DAPI with a much lower affinity, leaving dark regions within the nucleus.[31] TotaFAM colocalizes with the dark regions of the DAPI stain (Figure 4B), indicating that TotaFAM accumulates within nucleoli (Figure 4C,D). Tat peptides conjugated to low-molecular weight cargo have previously been demonstrated to localize to nucleoli within minutes.[32,33] TotaFAM accumulates in nucleoli but is also observed throughout the cell (Figure 4C).

Comparison of $^{13}$C DNP NMR spectra and $T_{1\_DNP}$ times to the TotaFAM enhanced data indicates cellular uptake of both AMUPol and sterically shielded monoradical. The short magnetization recovery time of the samples [$T_{1\_DNP}$ < 3 s (see Figure S11)] indicates the proximity of the radicals to the observed carbon nuclei and excludes the possibility that radicals polarize the carbon within the cells via long-range proton spin diffusion-mediated polarization from radicals not taken up by cells. Figure S10 shows virtually identical spectra of HEK293F cells in carbon free phosphate-buffered saline (PBS) and the standard MEM containing carbon, confirming the observed carbon resonances originate from the HEK293F cells. We note small differences in the $^{13}$C spectra recorded with the nitroxide monoradical and the biradicals. We attribute these minor differences to the amphiphilic nature of the nitroxide monoradical and expect an altered distribution of radical to both the cytosolic and membranous regions. Therefore, we conclude both AMUPol and the sterically shielded nitroxide monoradical are within the cells yet cannot currently determine their intracellular distribution.

To further characterize the performance of polarizing agents for in-cell DNP, we determined DNP enhancements using both AMUPol and TotaFAM at 2.7 mM. The TotaFAM DNP enhancement (63) was nearly twice as large as the AMUPol enhancement (35) (Figure 5). The AMUPol concentration

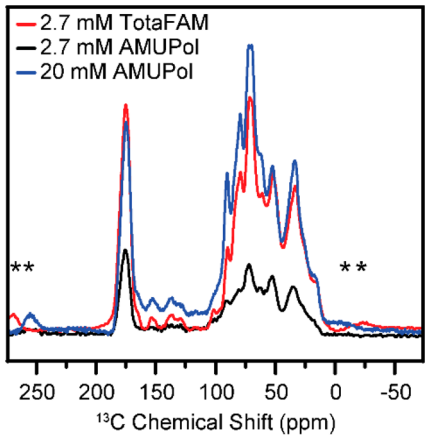


**Figure 5.** Comparison between DNP-enhanced spectra of HEK293F cells at <6 K with TotaFAM at 2.7 mM (red), AMUPol at 2.7 mM (black), and AMUPol at 20 mM (blue). Experimental details can be found in Table S1. Asterisks denote spinning side bands.

must be increased to 20 mM to yield similar enhancements. We note that AMUPol has previously been demonstrated to exhibit depolarization more extensive than that of Totapol, which decreases the intensity of the NMR signal recorded without microwave irradiation.[34] Therefore, the performance of TotaFAM compared to that of AMUPol is even better than indicated by the microwave on/off DNP enhancements we report (see Figure S8). We also note an observed lengthening of $^1$H $T_1$ to 6.7 s from 2.7 s when the TotaFAM radical concentration is decreased from 5.2 to 4.8 mM (see Figure S12). TotaFAM is therefore an effective polarizing agent for in-cell NMR, providing large DNP signal enhancements at relatively low concentrations. Lower concentrations of such targeted DNP polarizing agents[35] can be advantageous for decreasing associated cell toxicity.[36]

## CONCLUSIONS

We present MAS DNP employing trimodal polarizing agents to achieve significant DNP NMR signal enhancements within intact human cells. A novel trimodal fluorescent polarizing agent penetrates human cells, enables subcellular localization by fluorescence microscopy, and yields excellent DNP performance. DNP enhancements of 63 in human cells significantly increase the sensitivity of in-cell NMR, while access to sample temperatures of <6 K provides an additional 41-fold gain in NMR signal intensity compared to that at room temperature. Importantly, experiments can be repeated using a short delay (<3 s) for signal averaging. Together, these improvements in NMR sensitivity will decrease the required signal averaging time by multiple orders of magnitude, both for in-cell DNP and for *in vitro* sample preparations. DNP enhancements of >50 are observed below 6 K, and also at 90 K, a temperature regime that is readily accessible on commercially available DNP spectrometers. These promising results lay the foundation for developing polarizing agents and the methodology required to further improve DNP-enhanced in-cell NMR spectroscopy.

Trimodal polarizing agents provide a powerful localization method for studying molecular structures at atomic resolution within targeted cellular structures. Further customization of the three moieties of trimodal polarizing agents will maximize their utility. For example, peptide specificity can be tuned for further targeting of subcellular localization of DNP polarizing agents


DOI: 10.1021/acs.biochem.8b00257
*Biochemistry* 2018, 57, 4741–4746

within cells.[37] Furthermore, sterically shielded radicals will slow reduction inside cellular environments and allow for time intensive studies.[21,38] Employing sterically shielded radicals as DNP polarizing agents will also decrease cellular toxicity. Lastly, utilizing specialized fluorophores for super-resolution will enhance the optical resolution and provide more accurate subcellular localization.[39]

MAS DNP NMR at temperatures of <6 K greatly improves the capability of NMR to track the fate of metabolites, with important applications to metabolic flux analysis.[40,41] The intensities of NMR signals are increased by orders of magnitude, and the subcellular localization of the enhanced NMR signals can be determined using fluorescent polarizing agents. Therefore, through the advancements in DNP methodology and polarizing agents, we have established the experimental framework required to track cellular trafficking and chemical modifications of isotopically enriched metabolites. The advances demonstrated herein provide an impactful platform for future studies in endogenous environments and improved in-cell DNP.

## ■ ASSOCIATED CONTENT

### Supporting Information

The Supporting Information is available free of charge on the ACS Publications website at DOI: 10.1021/acs.biochem.8b00257.

Methods and additional data, including pulse sequences, NMR experimental parameters, synthetic routes, EPR, and mass spectrometry characterization (PDF)

## ■ AUTHOR INFORMATION


### Corresponding Author

*Department of Chemistry, Washington Univeristy in St. Louis, One Brookings Drive, St. Louis, MO 63130. E-mail: barnesab@wustl.edu. Phone: (617) 642-3225.

### ORCID

Faith J. Scott: 0000-0003-3903-8842

Snorri Th. Sigurdsson: 0000-0003-2492-1456

Alexander B. Barnes: 0000-0003-3748-8508


### Author Contributions

B.J.A., C.G., and E.L.S. contributed equally to this work.


### Funding

This research was supported by the National Institutes of Health (DP2-GM119131) and the National Science Foundation Instrument Development for Biological Research (CAREER DBI-1553577).


### Notes

The authors declare no competing financial interest.

## ■ ACKNOWLEDGMENTS


Confocal fluorescent imaging was performed in part through the use of the imaging facility of the Department of Biology of Washington University in St. Louis. The authors thank Seong Ho Pahng for useful discussion and Dr. Anil P. Jagtap for the preparation of the sterically shielded nitroxide monoradical used for the in-cell experiments.


## ■ REFERENCES


(1) Hoop, C. L., Lin, H.-K., Kar, K., Magyarfalvi, G., Lamley, J. M., Boatz, J. C., Mandal, A., Lewandowski, J. R., Wetzel, R., and van der Wel, P. C. A. (2016) Huntingtin exon 1 fibrils feature an interdigitated β-hairpin−based polyglutamine core. *Proc. Natl. Acad. Sci. U. S. A. 113*, 1546−1551.

(2) Tuttle, M. D., Comellas, G., Nieuwkoop, A. J., Covell, D. J., Berthold, D. A., Kloepper, K. D., Courtney, J. M., Kim, J. K., Barclay, A. M., Kendall, A., Wan, W., Stubbs, G., Schwieters, C. D., Lee, V. M. Y., George, J. M., and Rienstra, C. M. (2016) Solid-state NMR structure of a pathogenic fibril of full-length human α-synuclein. *Nat. Struct. Mol. Biol. 23*, 409−415.

(3) Zech, S. G., Wand, A. J., and McDermott, A. E. (2005) Protein Structure Determination by High-Resolution Solid-State NMR Spectroscopy: Application to Microcrystalline Ubiquitin. *J. Am. Chem. Soc. 127*, 8618−8626.

(4) Thongsomboon, W., Serra, D. O., Possling, A., Hadjineophytou, C., Hengge, R., and Cegelski, L. (2018) Phosphoethanolamine cellulose: A naturally produced chemically modified cellulose. *Science 359*, 334−338.

(5) Petkova, A. T., Ishii, Y., Balbach, J. J., Antzutkin, O. N., Leapman, R. D., Delaglio, F., and Tycko, R. (2002) A structural model for Alzheimer's β-amyloid fibrils based on experimental constraints from solid state NMR. *Proc. Natl. Acad. Sci. U. S. A. 99*, 16742−7.

(6) Selenko, P., Serber, Z., Gadea, B., Ruderman, J., and Wagner, G. (2006) Quantitative NMR analysis of the protein G B1 domain in Xenopus laevis egg extracts and intact oocytes. *Proc. Natl. Acad. Sci. U. S. A. 103*, 11904−11909.

(7) Theillet, F.-X., Binolfi, A., Bekei, B., Martorana, A., Rose, H. M., Stuiver, M., Verzini, S., Lorenz, D., van Rossum, M., Goldfarb, D., and Selenko, P. (2016) Structural disorder of monomeric α-synuclein persists in mammalian cells. *Nature 530*, 45−50.

(8) Sakakibara, D., Sasaki, A., Ikeya, T., Hamatsu, J., Hanashima, T., Mishima, M., Yoshimasu, M., Hayashi, N., Mikawa, T., Wälchli, M., Smith, B. O., Shirakawa, M., Güntert, P., and Ito, Y. (2009) Protein structure determination in living cells by in-cell NMR spectroscopy. *Nature 458*, 102−105.

(9) Inomata, K., Ohno, A., Tochio, H., Isogai, S., Tenno, T., Nakase, I., Takeuchi, T., Futaki, S., Ito, Y., Hiroaki, H., and Shirakawa, M. (2009) High-resolution multi-dimensional NMR spectroscopy of proteins in human cells. *Nature 458*, 106−109.

(10) Bah, A., Vernon, R. M., Siddiqui, Z., Krzeminski, M., Muhandiram, R., Zhao, C., Sonenberg, N., Kay, L. E., and Forman-Kay, J. D. (2015) Folding of an intrinsically disordered protein by phosphorylation as a regulatory switch. *Nature 519*, 106−109.

(11) Nguyen, V., Wilson, C., Hoemberger, M., Stiller, J. B., Agafonov, R. V., Kutter, S., English, J., Theobald, D. L., and Kern, D. (2017) Evolutionary drivers of thermoadaptation in enzyme catalysis. *Science (Washington, DC, U. S.) 355*, 289−294.

(12) Hackmann, A., Seidel, H., Kendrick, R. D., Myhre, P. C., and Yannoni, C. S. (1988) Magic-angle spinning NMR at near-liquid-helium temperatures. *J. Magn. Reson. 79*, 148−153.

(13) Boss, J. M., Cujia, K. S., Zopes, J., and Degen, C. L. (2017) Quantum sensing with arbitrary frequency resolution. *Science (Washington, DC, U. S.) 356*, 837−840.

(14) Bajaj, V. S., Mak-Jurkauskas, M. L., Belenky, M., Herzfeld, J., and Griffin, R. G. (2009) Functional and shunt states of bacteriorhodopsin resolved by 250 GHz dynamic nuclear polarization-enhanced solid-state NMR. *Proc. Natl. Acad. Sci. U. S. A. 106*, 9244−9.

(15) Hall, D. A., Maus, D. C., Gerfen, G. J., Inati, S. J., Becerra, L. R., Dahlquist, F. W., and Griffin, R. G. (1997) Polarization-Enhanced NMR Spectroscopy of Biomolecules in Frozen Solution. *Science (Washington, DC, U. S.) 276*, 930−932.

(16) Lange, S., Franks, W. T., Rajagopalan, N., Döring, K., Geiger, M. A., Linden, A., van Rossum, B. J., Kramer, G., Bukau, B., and Oschkinat, H. (2016) Structural analysis of a signal peptide inside the ribosome tunnel by DNP MAS NMR. *Sci. Adv. 2*, e1600379.

(17) Ardenkjaer-Larsen, J. H., Fridlund, B., Gram, A., Hansson, G., Hansson, L., Lerche, M. H., Servin, R., Thaning, M., and Golman, K. (2003) Increase in signal-to-noise ratio of > 10,000 times in liquid-state NMR. *Proc. Natl. Acad. Sci. U. S. A. 100*, 10158−10163.

(18) Kaplan, M., Cukkemane, A., van Zundert, G. C. P., Narasimhan, S., Daniëls, M., Mance, D., Waksman, G., Bonvin, A. M. J. J., Fronzes,




DOI: 10.1021/acs.biochem.8b00257
*Biochemistry* 2018, 57, 4741−4746

R., Folkers, G. E., and Baldus, M. (2015) Probing a cell-embedded megadalton protein complex by DNP-supported solid-state NMR. *Nat. Methods 12*, 649−652.
(19) Takahashi, H., Ayala, I., Bardet, M., De Paëpe, G., Simorre, J.-P., and Hediger, S. (2013) Solid-state NMR on bacterial cells: selective cell wall signal enhancement and resolution improvement using dynamic nuclear polarization. *J. Am. Chem. Soc. 135*, 5105−5110.
(20) Yamamoto, K., Caporini, M. A., Im, S.-C., Waskell, L., and Ramamoorthy, A. (2015) Cellular solid-state NMR investigation of a membrane protein using dynamic nuclear polarization. *Biochim. Biophys. Acta, Biomembr. 1848*, 342−349.
(21) Jagtap, A. P., Krstic, I., Kunjir, N. C., Hänsel, R., Prisner, T. F., and Sigurdsson, S. T. (2015) Sterically shielded spin labels for in-cell EPR spectroscopy: Analysis of stability in reducing environment. *Free Radical Res. 49*, 78−85.
(22) Sesti, E. L., Alaniva, N., Rand, P. W., Choi, E. J., Albert, B. J., Saliba, E. P., Scott, F. J., and Barnes, A. B. (2018) Magic Angle Spinning NMR Below 6 K with a Computational Fluid Dynamics Analysis of Fluid Flow and Temperature Gradients. *J. Magn. Reson. 286*, 1−9.
(23) Scott, F. J., Saliba, E. P., Albert, B. J., Alaniva, N., Sesti, E. L., Gao, C., Golota, N. C., Choi, E. J., Jagtap, A. P., Wittmann, J. J., Eckardt, M., Harneit, W., Corzilius, B., Sigurdsson, S. Th., and Barnes, A. B. (2018) Frequency-Agile Gyrotron for Electron Decoupling and Pulsed Dynamic Nuclear Polarization. *J. Magn. Reson. 289*, 45−54.
(24) Sauvée, C., Rosay, M., Casano, G., Aussenac, F., Weber, R. T., Ouari, O., and Tordo, P. (2013) Highly Efficient, Water-Soluble Polarizing Agents for Dynamic Nuclear Polarization at High Frequency. *Angew. Chem., Int. Ed. 52*, 10858−10861.
(25) Viennet, T., Viegas, A., Kuepper, A., Arens, S., Gelev, V., Petrov, O., Grossmann, T. N., Heise, H., and Etzkorn, M. (2016) Selective Protein Hyperpolarization in Cell Lysates Using Targeted Dynamic Nuclear Polarization. *Angew. Chem., Int. Ed. 55*, 10746−10750.
(26) Mann, D. A., and Frankel, A. D. (1991) Endocytosis and targeting of exogenous HIV-1 Tat protein. *EMBO J. 10*, 1733−9.
(27) Moulton, H. M., Nelson, M. H., Hatlevig, S. A., Reddy, M. T., and Iversen, P. L. (2004) Cellular Uptake of Antisense Morpholino Oligomers Conjugated to Arginine-Rich Peptides. *Bioconjugate Chem. 15*, 290−299.
(28) Hu, K.-N., Yu, H., Swager, T. M., and Griffin, R. G. (2004) Dynamic Nuclear Polarization with Biradicals. *J. Am. Chem. Soc. 126*, 10844−10845.
(29) Fontaine, S. D., Reid, R., Robinson, L., Ashley, G. W., and Santi, D. V. (2015) Long-term stabilization of maleimide-thiol conjugates. *Bioconjugate Chem. 26*, 145−152.
(30) Alley, S. C., Benjamin, D. R., Jeffrey, S. C., Okeley, N. M., Meyer, D. L., Sanderson, R. J., and Senter, P. D. (2008) Contribution of linker stability to the activities of anticancer immunoconjugates. *Bioconjugate Chem. 19*, 759−765.
(31) Pontvianne, F., Carpentier, M. C., Durut, N., Pavlištová, V., Jaške, K., Schořová, Š., Parrinello, H., Rohmer, M., Pikaard, C. S., Fojtová, M., Fajkus, J., and Sáez-Vásquez, J. (2016) Identification of Nucleolus-Associated Chromatin Domains Reveals a Role for the Nucleolus in 3D Organization of the A. thaliana Genome. *Cell Rep. 16*, 1574−1587.
(32) Silhol, M., Tyagi, M., Giacca, M., Lebleu, B., and Vivès, E. (2002) Different mechanisms for cellular internalization of the HIV-1 Tat-derived cell penetrating peptide and recombinant proteinsfused to Tat. *Eur. J. Biochem. 269*, 494−501.
(33) Tunnemann, G., Martin, R. M., Haupt, S., Patsch, C., Edenhofer, F., and Cardoso, M. C. (2006) Cargo-dependent mode of uptake and bioavailability of TAT-containing proteins and peptides in living cells. *FASEB J. 20*, 1775−1784.
(34) Mentink-Vigier, F., Paul, S., Lee, D., Feintuch, A., Hediger, S., Vega, S., and De Paëpe, G. (2015) Nuclear Depolarization and Absolute Sensitivity in Magic-Angle Spinning Cross-Effect Dynamic Nuclear Polarization. *Phys. Chem. Chem. Phys. 17*, 21824−21836.
(35) Rogawski, R., Sergeyev, I. V., Zhang, Y., Tran, T. H., Li, Y., Tong, L., and McDermott, A. E. (2017) NMR Signal Quenching from Bound Biradical Affinity Reagents in DNP Samples. *J. Phys. Chem. B 121*, 10770−10781.
(36) Stohs, S. J. (1995) The Role of Free Radicals in Toxicity and Disease. *J. Basic Clin. Physiol. Pharmacol. 6*, 205−228.
(37) Hoye, A. T., Davoren, J. E., Wipf, P., Fink, M. P., and Kagan, V. E. (2008) Targeting mitochondria. *Acc. Chem. Res. 41*, 87−97.
(38) Kocherginsky, N., and Swartz, H. M. (1995) *Nitroxide Spin Labels: Reactions in Biology and Chemistry*, CRC Press, Inc., Boca Raton, FL.
(39) Dempsey, G. T., Vaughan, J. C., Chen, K. H., Bates, M., and Zhuang, X. (2011) Evaluation of fluorophores for optimal performance in localization-based super-resolution imaging. *Nat. Methods 8*, 1027−1040.
(40) Chen, Y. J., Mahieu, N. G., Huang, X., Singh, M., Crawford, P. A., Johnson, S. L., Gross, R. W., Schaefer, J., and Patti, G. J. (2016) Lactate metabolism is associated with mammalian mitochondria. *Nat. Chem. Biol. 12*, 937−943.
(41) Chen, Y. J., Huang, X., Mahieu, N. G., Cho, K., Schaefer, J., and Patti, G. J. (2014) Differential incorporation of glucose into biomass during Warburg metabolism. *Biochemistry 53*, 4755−4757.


DOI: 10.1021/acs.biochem.8b00257
*Biochemistry* 2018, 57, 4741−4746